ELSEVIER

PII: S0011-2275(98)00083-6

Cryogenics **38** (1998) 1007–1015

Printed in Great Britain
0011-2275/98/$ - see front matter

Critical current density of superconductors as a function of strain in high magnetic fields

H.A. Hamid* and D.P. Hampshire

Department of Physics, University of Durham, South Road, Durham DH1 3LE, UK

Received 23 June 1998

A probe has been designed and built to measure the critical current density (J_C) of short superconducting wires and tapes as a function of strain (ϵ) in small bore high field magnets. The probe can measure currents of up to 100 Amps and strains of ± 1.0% on both low and high temperature superconductors. Measurements can be made in our 40 mm bore 17 T high magnetic field system in pumped cryogens. Strain is measured using commercial strain gauges pasted directly onto the samples. A Ag-sheathed $Bi_2Sr_2Ca_2Cu_3O_X$ tape has been measured at 4.2 K in magnetic fields up to 12 T. J_C is hysteretic in high magnetic fields and is weakly dependent on magnetic field and tensile strain up to ~ 0.29%. Beyond ~ 0.29% strain, the filaments break and J_C drops precipitously. Results are also presented for the effect of tensile and compressive strain for a 0.37 mm diameter Nb_3Sn wire at 4.2 K and 2.9 K from 10 T up to 14 T. The data confirm that a simple scaling law that includes the upper critical field ($B_{C2}(T,\epsilon)$) and the reduced field ($B/B_{C2}(T,\epsilon)$) alone cannot accurately describe the field, temperature and strain dependence of J_C.

Keywords: superconductors (A); critical current density (C); flux pinning (C); mechanical properties (C); critical field (C)

The effect of strain on the current carrying capacity (J_C) of superconducting tapes and wires is an important factor in their technological use. Superconducting magnet applications, for example, subject the conductor to strain on the order of 0.2% during the process from winding the conductor to forming a magnet[1]. For Nb_3Sn a tensile strain of 0.5% at 14 T can reduce its J_C by 50%[2]. Therefore, it is important to understand the strain tolerance of J_C in superconducting tapes and wires.

This paper describes the design and operation of a probe for use in small bore high field magnets. Variable temperature data are presented, obtained using pumped cryogens for both compressive and tensile strain. Tensile measurements on the high temperature superconductor (HTS) $Bi_2Sr_2Ca_2Cu_3O_X$ (BiSCCO) tape show that degradation of J_C is consistent with the filaments cracking at ~ 0.29%. By measuring the low temperature superconductor (LTS) Nb_3Sn at 4.2 K in tension and 2.9 K in compression, direct evidence is provided for the functional form of the field, temperature and strain dependence of J_C.

The next section outlines the principle of operation and design of the probe. There follows a description of how the superconducting sample is mounted onto the probe. Then a brief outline of the external circuitry and the procedure for taking data is described. The next three sections provide the critical current data for a BiSCCO tape and a Nb_3Sn wire and an analysis of these data. This is followed by a discussion of the performance of the probe and the experimental results. Finally, a short summary of the main findings is provided.

The strain probe

Principle of operation

The measurement procedure consists of attaching a strain gauge to the sample which is situated at the bottom of the probe. Current leads are attached to the sample together with two voltage taps at a distance of 3–5 mm apart. The strain gauge lies between the voltage taps. The probe is inserted into a high field magnet. Strain is applied to the sample via a gear system located at the top of the probe. The value of the strain is calculated from the change in resistance of the strain gauge. The transport current through the superconductor versus voltage across the taps (I–V) is measured as a function of magnetic field. Then the I–V measurements are repeated at the different values of strain required.

*To whom correspondence should be addressed

The construction of the probe

Figure 1 shows the overall construction of the strain probe. It uses a gear system to transfer the driving force from the top of the probe down to the sample operating in a similar way to a 'car-jack'. The gear system rotates the upper and lower rod. Because the lower brass struts are fixed by the pivot pin, the rotation moves the threaded end of the lower rod into the screwthread housing which lifts it towards the collar. This causes the upper brass struts at the bottom section of the probe to move upwards. This upward movement causes the top part of the lower brass struts to close which opens the bottom part of the lower brass struts. This movement stretches the sample. The upper and lower rod can be rotated clockwise for tensile measurements and anticlockwise for compressive measurements.

The collar is one of the fixed points in the probe. The fastening screws ensure the collar is anchored to the demountable stainless steel sheath. *Figure 2* shows the bottom section of the probe. The slot screw locates into a slot in the stainless steel rod and ensures the lower rod can rotate but cannot move up or down with respect to the collar. The upper brass struts are connected to the screwthread housing and the lower brass struts by stainless steel pins which are insulated using PTFE to reduce friction. The bottom part of each lower brass strut has two brass posts for sample mounting which are insulated with tufnol. The lower brass struts are attached to the demountable stainless steel sheath by inserting the stainless steel pivot pin which prevents the bottom section of the probe from rotating when strain is applied. The two halves of the lower brass struts are connected to each other by two springs which return the lower brass struts to their normal position when tension is removed.

The overall length of the probe is 1825 mm. The diameter of the probe is limited to 37 mm so that it can be inserted in the 40 mm bore of our Oxford Instruments 17 Tesla magnet. The top brass head consists of two electrical leadthroughs for current leads, two 10-pin connectors for instrumentation leads, a one-way valve and a gear system attached to an aluminium lifting bracket. A thin-walled demountable stainless steel sheath protects the instrumentation leads. It also helps to reduce heat loss and the overall weight of the probe.

The high current leads enter the middle section of the brass head via two vacuum-tight current leadthroughs (*Figure 1*). At this point they each consist of five pairs of

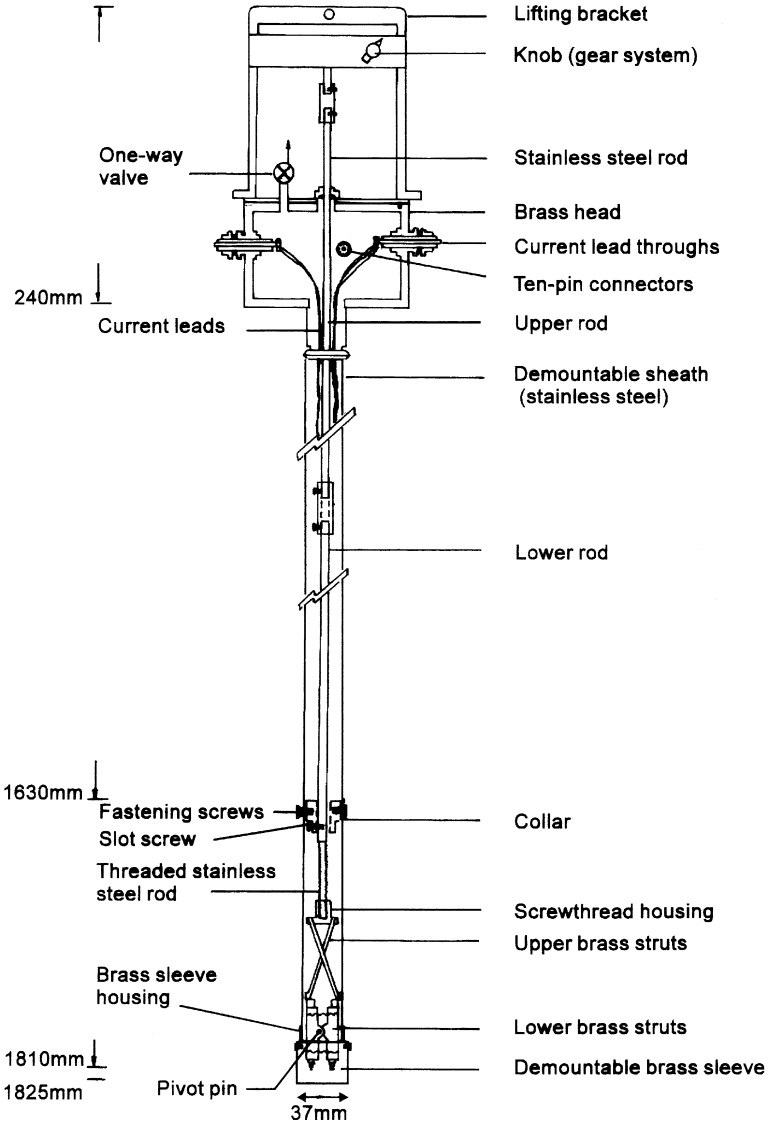

Figure 1 The strain probe (drawn to scale)

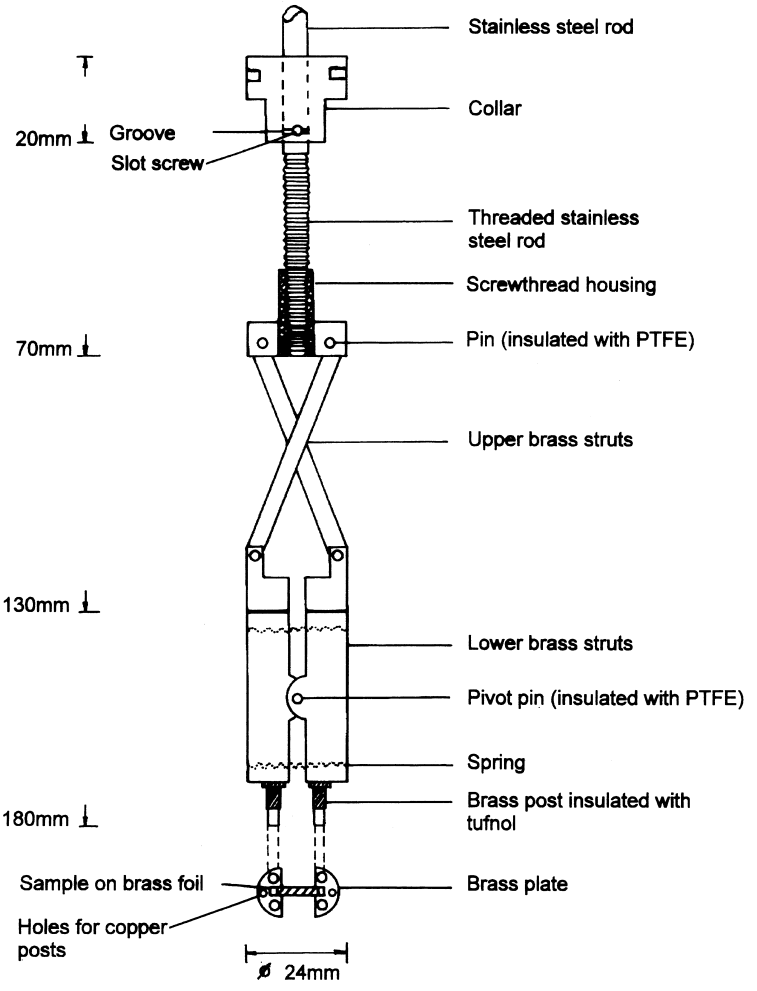

Figure 2 The bottom section of the strain probe (drawn to scale)

twisted copper wires of 0.71 diameter. Travelling down the probe the number of wires in the leads is reduced until there is only a single pair attached to the sample which reduces helium consumption. The current leads are electrically isolated from the main body of the probe by wrapping them with Mylar tape. Instrumentation leads are connected to two 10-pin connectors at the middle of the brass head. All instrumentation leads are twisted pairs to minimize electrical noise in high fields. Since the central rod rotates during strain measurements, enough slack is given to the instrumentation leads and the high current leads to cater for these rotations.

When high sample currents flow, the Joule heat produces cold helium gas. Some of this gas flows past the current leads through several holes in the stainless steel demountable sheath and out through the one-way valve at the brass head. These holes are placed below the line of the cryostat baffles. The gas flow prevents the current leads from overheating and also helps reduce helium consumption.

The whole system is leak-tight so that variable temperature measurements can be made from 4.2 K to 1.8 K in liquid helium using vapour pressure thermometry.

Sample mounting and strain measurements

The first series of experiments reported here were made on a multifilamentary $Bi_2Sr_2Ca_2Cu_3O_X$/Ag (BiSCCO) tape. It has a thickness 0.3 mm and a width 3.4 mm. The superconducting material makes up about 40% of its cross-sectional area. It was fabricated using the oxide-powder-in-tube technique. The second series of experiments were made on a bronze route 0.37 mm diameter, Nb_3Sn multifilamentary wire which consists of 4500 Nb filaments in a bronze matrix. The superconducting Nb_3Sn layer was formed using a heat treatment of 700°C for 64 h.

Before starting a series of measurements, the demountable stainless steel sheath is temporarily removed to check the instrumentation leads inside the probe. The pivot pin is inserted and the sample assembly, which includes the strain gauge, is attached to the brass plates across the lower brass struts. It is critical to mount the sample assembly properly to obtain correct results. The procedures for making the sample assembly for the BiSCCO tape and the Nb_3Sn wire are described below.

BiSCCO sample assembly

The HTS tape was cut to about 9 mm long. A commercial strain gauge (Micro-Measurements: WK-06-062AP-350) was reduced to 4.5 × 2 mm by removing some of the surrounding backing material. The manufacturers procedure was used to mount the strain gauge directly onto the tape between the voltage taps. After curing at 100°C for 4 h, the sample was soldered onto a 3.5 × 10 × 0.1 mm brass foil. We found by trial and error that a foil thickness of 0.1 mm was required to support the tape. With thinner foils the tape broke prematurely. With thicker foils unacceptably large

driving forces were required to produce the required strain. PbSnAg solder (Fibra-Sonics S-100A-10) was used for sample mounting rather than ordinary PbSn solder. The PbSnAg solder has a melting point of 305°C and is more ductile at low temperatures[3]. The tape/foil was soldered onto the brass plates at the bottom end of the probe. For tensile measurements, an additional 0.45 mm diameter copper wire was soldered to the brass posts which were electrically insulated from the tape with tufnol. Finally, the current leads and voltage taps were soldered directly to ends of the sample. This 'wire and foil' helped to extend the range of strain to well above the required 0.3% before the sample assembly broke.

Nb_3Sn sample assembly

It is essential that the sample is as straight as possible when the strain measurements are made. A steel holder which consisted of a recess to contain the sample was used when the sample was reacted (64 h at 700°C). The sample was coiled at both ends of a straight section ~ 9 mm long. A small commercial strain gauge (Micro-Measurements, type: EA-06-015DJ-120) was reduced in dimensions to 2.5 × 0.6 mm by cutting away some of its backing material. The strain gauge was pasted directly onto the wire and held in place around the wire using nylon string during curing (100°C for 4 h). Two copper posts were soldered into the holes on the brass plates. A 20 × 3 × 0.1 mm brass foil with holes to accept the posts was soldered across the plates. The Nb_3Sn sample was then soldered along its entire length onto the foil/plates so that the coiled ends of the sample surrounded the copper posts. The coiled ends increased the length for current transfer into the superconductor. Solder was very sparingly used along the straight length of the sample. The sample assembly (sample/foil/posts/plates) was fitted to the brass posts at the bottom of the probe as shown in *Figure 2*. The current leads were attached directly to the copper posts, the voltage taps to the sample and the instrumentation leads connected to the strain gauge terminals.

Strain measurements

After the sample has been mounted on the probe, the contraction of the probe when cooled to 4.2 K can strain the sample. In order to account for this, the resistance of a set of strain gauges mounted on the BiSCCO and the Nb_3Sn samples, and then freely suspended in liquid Helium was measured. These resistance readings were used to define the zero strain values in this paper. The uncertainty in the zero strain value from one sample/strain gauge to another was ± 0.02% for the Nb_3Sn wire, and for the BiSCCO tape ± 0.04%.

During each I–V measurement, the change in strain of the sample due to the Lorentz force was monitored and found to be less than 0.025%. When all the V–I traces were completed as a function of field, the strain reading typically returned to within 0.03% of its original value. The sensitivity of the strain measurement detected by the DMM is 1.4×10^{-4}% for the tape and 4.0×10^{-4}% for the wire. The control for changing the strain was typically 0.01% for the wire and 0.005% for the tape. We suggest the control is limited by slippage in the gearbox system when the sample is subjected to high strains, friction in the joints in the probe, and/or cracking in the solder.

Having measured more than 10 samples using the probe, sometimes when the upper and lower rod were rotated clockwise, the sample compressed rather than stretched. We attributed this to differential thermal contraction between various components of the probe. This problem did not compromise the data because the strain gauge was directly attached to the sample between the voltage taps.

After the sample has been mounted and the instrumentation leads connected, the demountable brass sleeve is attached to the probe to protect the sample while the probe is inserted into the magnet.

External circuitry

Figure 3 represents external circuitry and equipment for strain measurements. The constant current through the strain gauge is supplied from a Lakeshore 120 current source. The voltage across the strain gauge is detected by a Keithley DMM (voltmeter 1). The system is computer controlled by interactive, real time graphical software written using ASYST to take the V–I traces.

The sample current is generated either by a 100 Amp Thor Power Supply or by a 500 Amp Power Supply built in-house. The sample current is ramped by a Kepco voltage programmer and measured by a Keithley digital multimeter (voltmeter 2) using a standard resistor (c) in series. The sample voltage is measured using a Keithley 182 digital nanovoltmeter. Communication is by the IEEE bus for all instruments except for the magnet power supply which is connected by the RS232 bus.

Experimental results

J_C *for BiSCCO*

Figure 4 shows J_C versus tensile strain for the BiSCCO tape at 4.2 K at different fields. J_C is calculated using the cross-sectional area of the superconductor alone. The field was applied perpendicularly to both the direction of transport current and the flat surface of the tape (i.e. *B* parallel to the c-axis of the tape). These data were deduced from V–I traces using a 1.0 μV criteria (equivalent to 3 μV cm^{-1}) to ensure good signal to noise. The data starts at about 0.05% strain indicating that the tape was strained on cool-down by the probe. The figure shows that J_C is almost independent of strain from 0.05% to about ~ 0.29%. Above ~ 0.29% strain, J_C starts to decrease dramatically. After J_C has decreased to less than half its original value, the strain measured between the taps decreased. This is due to inhomogeneity in the mechanical properties of the tape which is discussed below. Consistent with this explanation, three other short samples from the same tape were measured (not presented in this paper). One sample showed similar properties to those reported in *Figures 4* and *5*. The other two samples showed an initial degradation in J_C at much lower strains of 0.05% and 0.1% followed by further decreases in J_C as the strain was increased.

Figure 5 shows that J_C is hysteretic with magnetic field. J_C is higher in decreasing fields than in increasing fields. This type of hysteresis has been observed before[4]. We attribute the anomalous hysteresis at 0.5 T at the high strain of 0.297% to filament breakage during the in-field measurements.

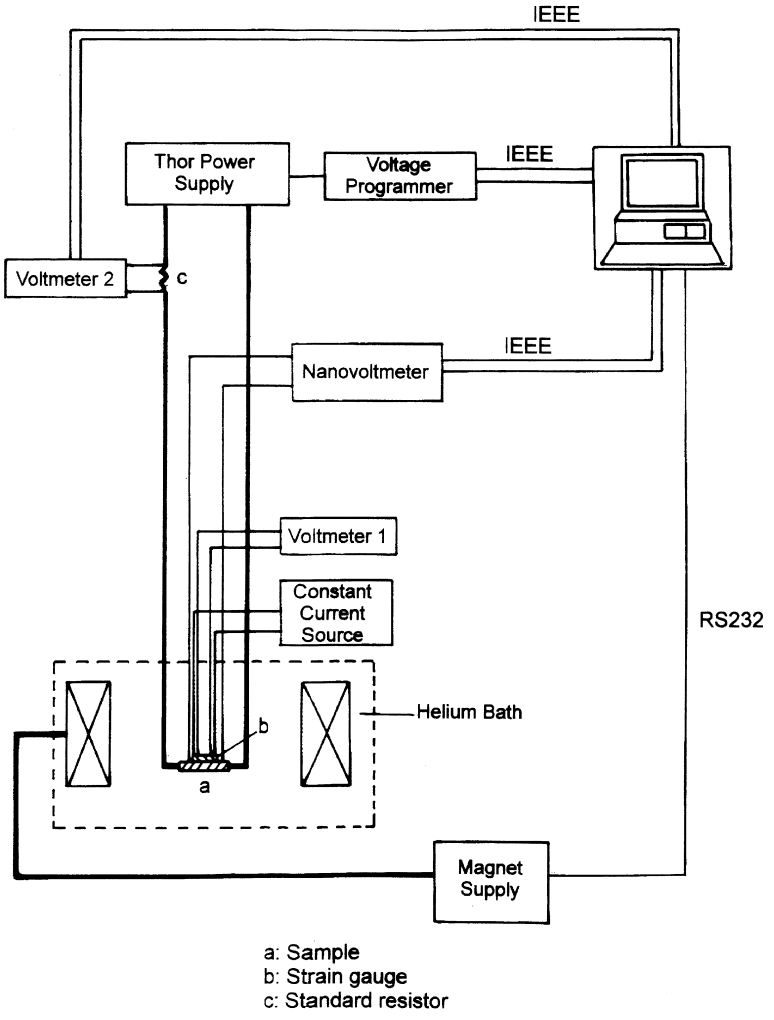

Figure 3 External circuitry and equipment for strain measurements

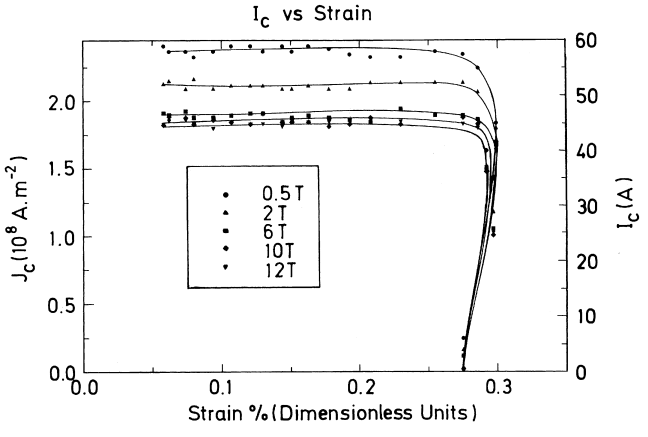

Figure 4 J_C versus tensile strain in high fields at 4.2 K for a BiSCCO tape

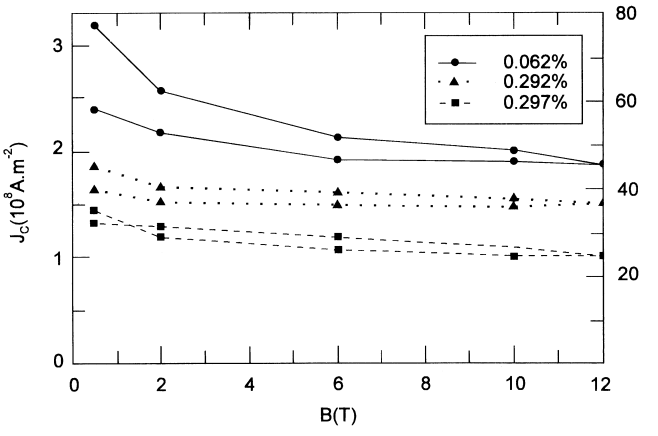

Figure 5 The hysteresis of J_C versus magnetic field at 4.2 K at three different strains for a BiSCCO tape. The J_C values are higher when the field has been decreased to the required value rather than increased

J_C for Nb_3Sn

Figure 6 shows the typical E–J characteristics for the Nb_3Sn wire. The strain value starts at about 0.1%. At low currents, there is a resistive baseline which can be attributed to current transfer. Because the sample is so short not all the current has transferred into the superconducting filaments between the voltage taps[5]. We have chosen a relatively high criterion of 10 μV (~ 25 μV cm^{-1}) to define J_C, to avoid errors associated with current transfer. The values of J_C quoted are for the entire cross-sectional area of the wire. *Figure 6* shows that as the strain increases from 0.1% to 0.2%, J_C increases. *Figure 7* shows the dependence of J_C in-field on tensile strain for the Nb_3Sn wire at 4.2 K. J_C reaches a peak value at about 0.25% and then decreases. For currents above ~ 90 Amps, the data are unreliable because the sample quenches. In *Figure 8*, the magnetic field and strain dependence of J_C for a second sample measured in compression at 2.9 K is shown. For these measure-

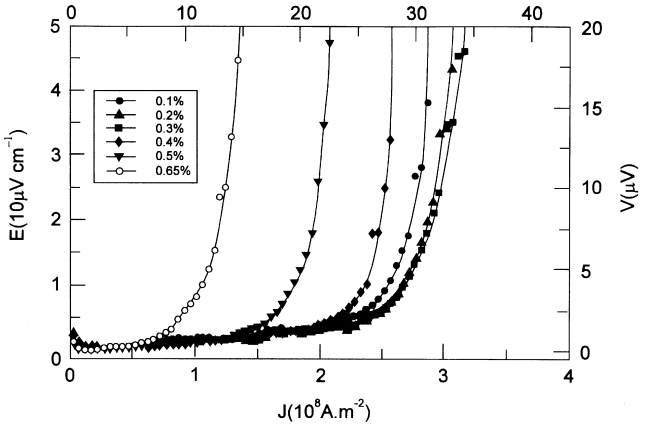

Figure 6 *E–J* data at 14 T and 4.2 K for Nb_3Sn at different values of strain

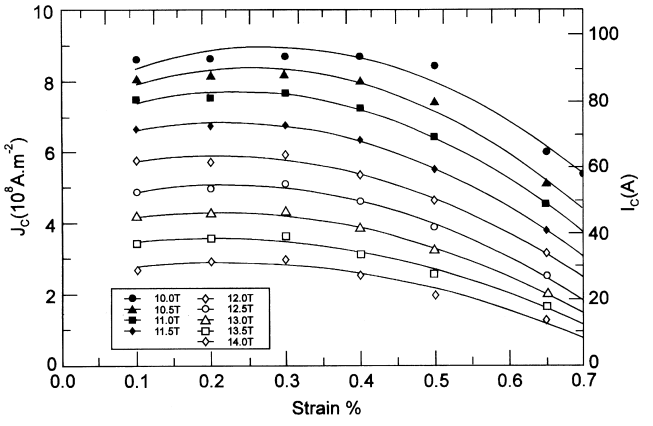

Figure 7 J_C versus tensile strain in high fields at 4.2 K for a Nb_3Sn wire: sample 1

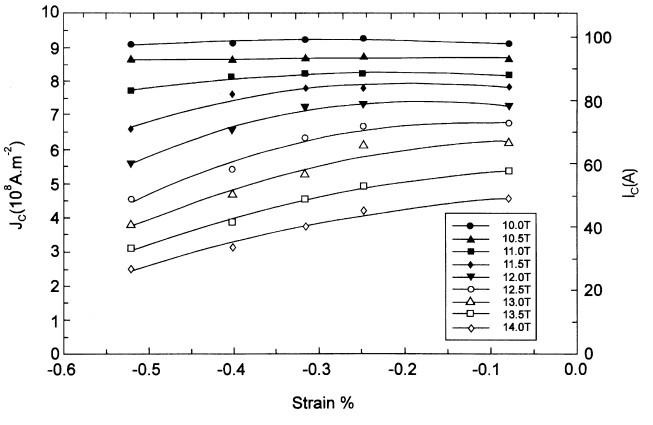

Figure 8 J_C versus compressive strain in high fields at 4.2 K for a Nb_3Sn wire: sample 2

ments made at low pressure, the sample quenches at currents above ~ 80 Amps.

The Kramer dependence in Nb_3Sn

The Scaling Laws in the literature which parametrize the volume pinning force F_P can be written in the form:

$$F_P = \alpha(T,\epsilon)b^p(1-b)^q \qquad (1)$$

where $\alpha(T,\epsilon)$ is a function of temperature, strain and the microstructure of the sample; p and q are constants and the

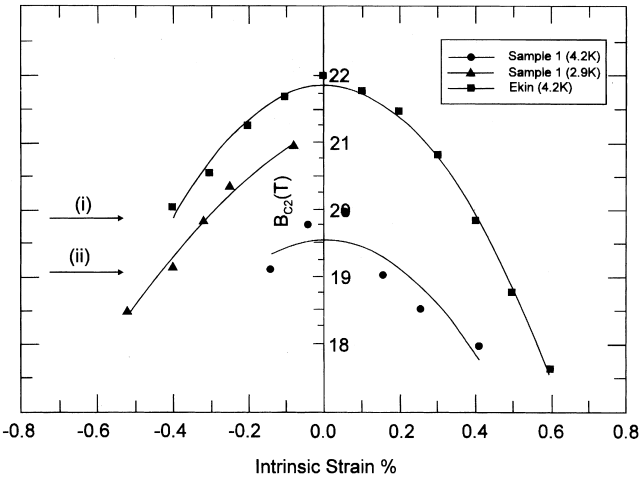

Figure 9 The upper critical field (B_{C2}) as a function of intrinsic strain for the two Nb_3Sn samples at 4.2 K. For comparison the data by Ekin[8] on doped Nb_3Sn is included. The arrows denote data sets where (i) B_{C2} = 19.1 T and (ii) B_{C2} = 19.8 T

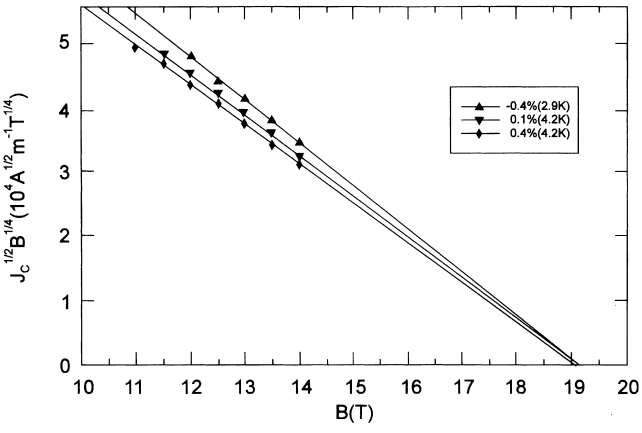

Figure 10 A Kramer plot: $J^{1/2}{}_CB^{1/4}$ versus B for Nb_3Sn. Data are taken for sample 1 at 4.2 K, 0.1% strain and 0.4% strain and for sample 2 at 2.9 K, – 0.4% strain

reduced field $b = B/B_{C2}$ where B_{C2} is the upper critical field. The Fietz–Webb Temperature Scaling Law[6] replaces $\alpha(T,\epsilon)$ by $\alpha B^n{}_{C2}$ (α is a constant). For Nb_3Sn and its ternaries, it is found experimentally that the Kramer law[7] operates where $p = 1/2$ and $q = 2$. Equation (1) can then be rearranged to give:

$$J_C^{1/2}B^{1/4} = \alpha^{1/2}B_{C2}^{\frac{n-5}{2}}(B_{C2}-B) \qquad (2)$$

By replotting the data in *Figures 7* and *8* on a Kramer plot (i.e. $J_C{}^{1/2}B^{1/4}$ versus B), a straight-line least-squares fit to the data at each temperature gives values of B_{C2}. In *Figure 9*, the calculated values of B_{C2} are presented for the Nb_3Sn measured in tension at 4.2 K and in compression at 2.9 K as a function of intrinsic strain. The intrinsic strain is defined to be zero when B_{C2} is at its peak value. The precompression is ~ 0.25%. For comparison, data by Ekin[8] for a doped Nb_3Sn compound are presented. Arrows in *Figure 9* highlight that a value of B_{C2} of either ~ 19.1 T or ~ 19.8 T can be found at three different values of strain and temperature. In *Figure 10*, a Kramer plot for the three data sets giving a value for B_{C2} of ~ 19.1 T are presented. It is apparent that despite the values of B_{C2} being approximately the same, the gradient of the lines are different. Similarly,

the data sets plotted on a Kramer plot in *Figure 11* show a similar value of B_{C2} and quite different gradients. For comparison, Kramer plots calculated from the data in Ekin's work[8] (*Figure 2*) are shown. Ekin's data at 4.2 K and our data at 4.2 K and 2.9 K are consistent with each other. When B_{C2} is lowered by applying strain, the magnitude of the gradient of the Kramer line increases.

Discussion

The strain probe

The design and operation of the strain probe has advantages:

1. the probe can fit into any magnet of bore size greater than 40 mm;
2. tensile and compressive strain can be measured;
3. very small strain can be applied to the sample by use of the gear system;
4. it is possible to measure the change in strain of the sample during measurements resulting from the Lorentz force; and
5. variable temperature data can be obtained using vapour pressure thermometry.

The limitations include:

1. only short samples can be measured. This leads to the current transfer length problem and to sample heating with high transport currents; and
2. the success of the measurements is very sensitive to how well the sample is mounted onto the probe.

Probes used by other workers

One of the most successful apparatuses designed to make strain measurements on superconductors was reported by Ekin[8]. The sample length measured was approximately 16.5 mm. Strains in excess of 1% were applied and measured using a strain gauge extensometer. This system was not designed to measure both tensile and compressive strains. Ekin has extensively analysed strain data in the context of the Scaling Laws which are discussed below. Haken[9] has used U-shaped bending springs, designed to measure tensile and compressive strains. Strain is applied by exerting a force to the legs of the U-shaped spring. The springs were made from brass because it has a low Young's modulus (95–100 GPa) and is simple to machine and easy to solder. However, these brass springs are massive and a large driving force is needed to apply strain. The strain range for this system is ± 1.2%. Haken has investigated the role of deviatoric strain in determining the critical parameters of superconductors.

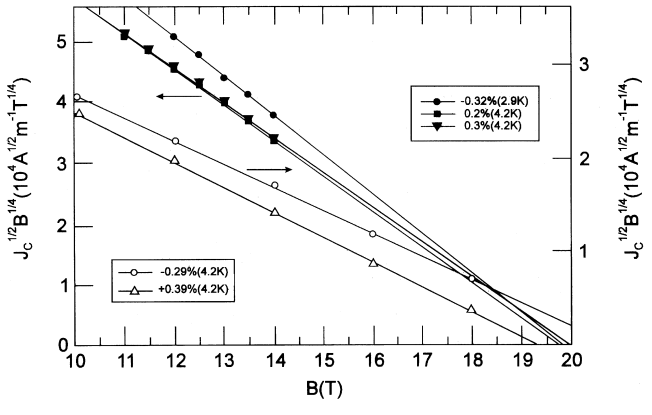

Figure 11 A Kramer plot: $J^{1/2}{}_CB^{1/4}$ versus B for Nb_3Sn. Sample 1 at 4.2 K, 0.2% strain and 0.3% strain and for sample 2 at 2.9 K, – 0.32% strain (left-hand axis). Data are also shown from Ekin[8] at 4.2 K at – 0.29% strain and + 0.39% strain (right-hand axis)

An elaborate description of a spiralled bending spring method was given by Walters[10]. This system was designed for tensile and compressive strains. In its original form, the system requires quite a large bore size magnet, approximately 55 mm. Since the sample is supported by a spring, the spring material must have a greater elastic limit than the maximum required for the measurements. Walters used 318 titanium alloy to meet this requirement. The disadvantage of this alloy is that it is difficult to solder the sample onto it. However, an important advantage of this probe is that it can be used to measure very high transport currents.

BiSCCO tape

The effect of strain on the J_C values for the BiSCCO tape presented in this work is consistent with the literature. It should be borne in mind that the precompression for Ag sheath BiSCCO is calculated to be 0.04%[11]. The effect of strain on J_C is very small at 4.2 K. Our current understanding of flux pinning mechanisms that determine J_C suggests that this result is consistent with very large values of B_{C2} for BiSCCO which suggests that high field measurements at high temperatures will be informative[12].

The degradation of J_C above 0.29% shown in this work is irreversible and consistent with the brittle filaments breaking. The variation in the strain tolerance of J_C in the other short samples measured shows that the mechanical properties of the BiSCCO tape are not uniform on the scale of the spacing between the voltage taps—a few millimetres. Necessarily, crack propagation is first initiated in the poorer sections of the tape. The remaining sections then contract until the Ag matrix adjacent to the crack has work hardened to sustain the applied stress[13]. Hence, the reduction in strain as J_C decreases shown in *Figure 4* suggests that cracks were first initiated outside of the voltage taps in a section with poorer mechanical properties. The insensitivity of J_C to strain up to 0.3% at the 3 μV cm^{-1} electric field criterion is for the section with better mechanical properties and is more likely to represent intrinsic properties of BiSCCO. Such properties may be achieved over long lengths as the homogeneity of the tapes is improved. At very low electric fields (~ 10 nV cm^{-1}), a residual resistivity has been reported in other BiSCCO tapes[14]. Further measurements are required to determine the strain tolerance of J_C at such low electric fields where current transfer into and out of the Ag matrix and microcracks play an important role[15,16].

Effort is being made worldwide to improve the mechanical properties of the BiSCCO tapes. It has been shown that the strain tolerance is increased by using a multifilamentary configuration[17–19]. Equally, by reducing the filament thickness from 20 μm to less than 5 μm, the strain at which cracks start to occur is increased from 0.2% to 1.0%[13]. Dispersion hardening the Ag matrix can also improve the strain properties of the BiSCCO. Another method which improves the strain tolerance of the BiSCCO tape is to co-process

the BiSCCO powder with Ag powder. With this fabrication route, the Ag powder acts as a crack arrestor[20].

Nb_3Sn tape

Ekin[8] found experimentally that the strain dependence of the upper critical field at 4.2 K can be parametrized by:

$$B_{C2}(\epsilon) = B_{C2}(\epsilon = \epsilon_m)(1 - a|\epsilon - \epsilon_m|^u) \quad (3)$$

where a, u, and ϵ_m are constants. ϵ is the applied strain and ϵ_m is the strain at which B_{C2} is a maximum. He found a strain scaling law of the form:

$$F_P = \alpha' B^m_{C2}(\epsilon) b^p (1 - b)^q \quad (4)$$

where α' is a constant. In general, the value of m in the strain scaling law is not the same as n in the Fietz–Webb Temperature Scaling Law. For example, the variable strain data at 4.2 K suggest that for NbTi, Nb_3Sn and V_3Ga, m is 4, 1.0 and 1.4, respectively[21]. However, the variable temperature data gave values for n of 2^{22}, 2^{23} and 3^{24}, respectively. Because the values of m and n are not the same, $\alpha(T,\epsilon)$ cannot be written in the form $\alpha^* B^n{}_{C2}(T,\epsilon)$($\alpha^*$, n constants). The variable-temperature variable-strain data in *Figures 10* and *11* provide experimental confirmation that the gradient of the Kramer plots is not uniquely determined by the value of B_{C2}. Were $\alpha(T,\epsilon)$ of the form $\alpha^* B^n{}_{C2}(T,\epsilon)$, if the upper critical field were increased (for example, by reducing the temperature) and then decreased back to its original value (for example by increasing the strain), the gradient of the Kramer plot should be unchanged. The experimental results in *Figures 10* and *11* do not show such behaviour.

Ekin proposed a general scaling law to unify the temperature and strain scaling results of the form:

$$F_P = \alpha''(1 - a|\epsilon - \epsilon_m|^u)^m (1 - t^2)^n b^p (1 - b)^q \quad (5)$$

where α'' is a constant and $t = T/T_C(\epsilon)$. The first term in brackets has been included to account for strain scaling and the second for temperature scaling. The implicit assumption underlying Ekin's law is that $\alpha(B,T)$, at least to a reasonable approximation at 4.2 K, is of a separable variable form in temperature and strain. This assumption awaits experimental confirmation.

Historically, the Fietz–Webb Scaling Law has provided the central framework to describe flux pinning. It allows the scaling of a limited data set to predict the general functional form. The results in this work confirm that a simple scaling law which includes $B_{C2}(T,\epsilon)$ and the reduced field (b) alone, cannot accurately describe the field, temperature and strain dependence of J_C. Model calculations of F_P for many pinning functions show that F_P depends on the Ginzburg–Landau parameter (κ)[25]. It is currently not known whether the strain and temperature dependence of κ is also of separable variable form which could resolve the discrepancy between the experimental data and model pinning calculations. Alternatively more complex pinning calculations or non-pinning mechanisms[26] may need to be considered.

Concluding remarks

Real progress in the application of superconducting materials depends on the understanding of their mechanical properties such as the effect of strain on J_C of these materials. Experiments range from simple bending tests to those involving complicated strain apparatus. The design and construction of a strain probe capable of measuring tensile and compressive strain and its effect on J_C has been presented. The probe can measure strains up to ± 1.0% on LTS and HTS wires and tapes. Strain is measured via a strain gauge pasted directly on the sample. The probe can be inserted into any magnet system with a bore size greater than 40 mm. The maximum current that can be passed through the probe is about 100 Amps. J_C versus strain measurements can be made using vapour pressure thermometry in Helium or Nitrogen.

For a BiSCCO tape, it has been found that J_C is hysteretic in high magnetic fields and is weakly dependent on magnetic field and strain up to 0.29% at 4.2 K. Beyond 0.29% strain, the filaments break and J_C drops precipitously.

For a Nb_3Sn wire, J_C has been measured as a function of strain at 4.2 K and 2.9 K in high magnetic fields. Consistent with the form of Ekin's proposed scaling law[8], the results in this work confirm that a simple scaling law which includes $B_{C2}(T,\epsilon)$ and the reduced field ($b = B/B_{C2}(T,\epsilon)$) alone, cannot accurately describe the field, temperature and strain dependence of J_C.

Acknowledgements

The authors wish to thank P. Armstrong and G. Teasdale for technical support, P. Russell for help with production of the figures, N. Cheggour, S. Keys and D. N. Zheng for useful discussions, MARA Institute of Technology (Malaysia) and the EPSRC UK. We thank D. Phillips from IGC, USA and M. Dietrich from Vacuumschmelze, Germany for supplying the samples.

References

1. Ekin, J. W., Finnemore, D. K., Li, Q., Tenbrink, J. and Carter, W., *Appl. Phys. Lett.*, 1992, **61**(7), 858.
2. Ekin, J. W., *IEEE Trans. Magn. MAG-19*, 1983, **3**, 900.
3. Warren, W. H. and Bader, W. G., *Rev. Sci. Instrum.*, 1969, **40**, 180.
4. Marti, F., Grasso, G., Huang, Y. and Flukiger, R., *IEEE Trans. Magn.*, 1997, **7**(2), 2215.
5. Ekin, J. W., *J. Appl. Phys.*, 1978, **49**, 3406.
6. Fietz, W. A. and Webb, W. W., *Phys. Rev.*, 1969, **178**, 657.
7. Kramer, E. J., *J. Appl. Phys.*, 1973, **44**(3), 1360.
8. Ekin, J. W., *Cryogenics*, 1980, **20**, 611.
9. Haken, B. T., PhD thesis, University of Twente Enchede, The Netherlands, 1994.
10. Walters, C. R., Davidson, I. M. and Tuck, G. E., *Cryogenics*, 1986, **26**, 406.
11. Keβler, J. and Goldacker, W., *Applied Superconductivity*, ed. H. C. Freyhardt. DGM Informationsgesellschaft Verlag, Oberursel, 1993, p. 213.
12. Richens, P. E., Jones, H., Van Cleemput, M. and Hampshire, D. P., *IEEE Trans. Magn.*, 1984, **21**, 289.
13. Suenaga, M., Fukumoto, Y., Haldar, P., Thurston, T. R. and Wildgruber, U., *Appl. Phys. Lett.*, 1995, **67**, 3025.
14. Fukumoto, Y., Li, Q., Wang, Y. L., Suenaga, M. and Haldar, P., *Appl. Phys. Lett.*, 1995, **66**, 1827.
15. Polak, M., Parrell, J. A., Polyanskii, A. A., Pashitski, A. E. and Larbalestier, D. C., *Appl. Phys. Lett.*, 1997, **70**, 1034.
16. Polak, M., Zhang, W., Parrell, J., Cai, X. Y., Polyanskii, A., Hellstrom, E. E., Larbalestier, D. C. and Majoros, M., *Super Sci. and Tech.*, 1997, **10**, 769.

17. Kirk-Othmer, *Encyclopedia of Chemical Technology*. Wiley, 1995.
18. Reed, R. P. and Clark, A. F., *Materials at Low Temperatures*. American Society for Metals, Metal Park, Ohio, 1983.
19. Friend, C. F., PhD thesis, Hatfield College University of Durham, Duram, 1994.
20. Dally, J. W., Riley, W. F. and McConnel, K. G., *Instrumentation for Engineering Measurements*. New York, Wiley, 1993.
21. Ekin, J. W., *IEEE Trans. Magn.-17*, 1981, p. 658.
22. Friend, C. M. and Hampshire, D. P., *Applied Superconductivity*, ed. H. C. Freyhardt. DGM Informationsgesellschaft Verlag, Oberursel, 1993, p. 23.
23. Hampshire, D. P., Jones, H. and Mitchell, E. W. J., *IEEE Trans. Magn.*, 1984, **21**, 289.
24. Hampshire, D. P., Clark, A. F. and Jones, H., *J. Appl. Phys.*, 1989, **66**, 3160.
25. Dew-Hughes, D., *Philos. Mag.*, 1974, **30**, 293.
26. Hampshire, D. P., *Physica C*, 1998, **296**, 153.